Theoretical considerations and empirical predictions of the pharmaco- and population dynamics of heteroresistance

Bruce R. Levin[a,b,1] ⓘD, Brandon A. Berryhill[a,c] ⓘD, Teresa Gil-Gil[a] ⓘD, Joshua A. Manuel[a] ⓘD, Andrew P. Smith[a], Jacob E. Choby[b,d] ⓘD, Dan I. Andersson[e] ⓘD, David S. Weiss[b,f,g], and Fernando Baquero[h] ⓘD

Antibiotics are considered one of the most important contributions to clinical medicine in the last century. Due to the use and overuse of these drugs, there have been increasing frequencies of infections with resistant pathogens. One form of resistance, heteroresistance, is particularly problematic; pathogens appear sensitive to a drug by common susceptibility tests. However, upon exposure to the antibiotic, resistance rapidly ascends, and treatment fails. To quantitatively explore the processes contributing to the emergence and ascent of resistance during treatment and the waning of resistance following cessation of treatment, we develop two distinct mathematical and computer-simulation models of heteroresistance. In our analysis of the properties of these models, we consider the factors that determine the response to antibiotic-mediated selection. In one model, heteroresistance is progressive, with each resistant state sequentially generating a higher resistance level. In the other model, heteroresistance is non-progressive, with a susceptible population directly generating populations with different resistance levels. The conditions where resistance will ascend in the progressive model are narrower than those of the non-progressive model. The rates of reversion from the resistant to the sensitive states are critically dependent on the transition rates and the fitness cost of resistance. Our results demonstrate that the standard test used to identify heteroresistance is insufficient. The predictions of our models are consistent with empirical results. Our results demand a reevaluation of the definition and criteria employed to identify heteroresistance. We recommend that the definition of heteroresistance should include a consideration of the rate of return to susceptibility.

microbiology | heteroresistance | antibiotic resistance | pharmacodynamics | mathematical modeling

Significance

This mathematical modeling and computer-simulation study quantitatively explores two broadly different, previously undescribed, classes of heteroresistance. In our analysis of the properties of these models, we consider the response of heteroresistant populations to antibiotic exposure, focusing on the conditions where heteroresistance could lead to clinical treatment failure. We also provide consideration to the rate of reversion from a resistant to a sensitive state. Our analysis illustrates the need to include the reversion rate from resistant to sensitive in the definition of heteroresistance and questions the sufficiency of the method currently used to identify heteroresistance.

Pathogens resistant to existing antibiotics are a significant and increasing source of morbidity and mortality for humans and domestic animals (1, 2). Fundamental to the effective treatment of bacterial infections is choosing an antibiotic to which the pathogen is susceptible. The level of susceptibility is readily estimated by culture methods, both through automation via BioMerieux's VITEK and similar devices (3–6) as well as by nonautomated methods such as disk diffusion and Epsilon-diffusion tests (7, 8). By these methods, bacteria are classified as susceptible, intermediate, or resistant according to the international consensus guidelines from the Clinical and Laboratory Standards Institute (CLSI) and the European Committee on Antimicrobial Susceptibility Testing (EUCAST). These categorical descriptions determine whether an antibiotic will or will not be used for treatment. If an isolate appears susceptible to an antibiotic by these criteria, the drug would be presumed to be effective in treating infections with that pathogen. These in vitro susceptibility estimates are not sufficient as measures of antibiotic susceptibility if the treated bacteria are heteroresistant to that drug.

A population of bacteria which is heteroresistant often appears susceptible to an antibiotic as assessed by the standard methods described above but quickly becomes resistant upon confrontation with that drug due to the selection for and ascent of minority-resistant populations. Heteroresistance (HR) is typically defined in an operational manner by the presence of one or more subpopulations at a frequency greater than 10^{-7} with a resistance level that crosses the breakpoint at or greater than 8 times the susceptible main population (9). The canonical test for the presence of these subpopulations, and thus for HR, is a Population Analysis Profile (PAP) test (10, 11). This protocol tests for bacterial growth at different concentrations of an antibiotic, thus revealing the presence or absence of resistant subpopulations.

HR is clinically and epidemiologically problematic due to the inherent instability of resistance. Within short order of the removal of the antibiotic, heteroresistant populations once again appear susceptible to the treating antibiotic by conventional testing procedures. This effect is most profound when considering the transmission of heteroresistant populations

between individuals. Patients with heteroresistant infections transmit these seemingly antibiotic-susceptible bacteria to other patients, who may then fail treatment with the drug for which the bacteria are heteroresistant. This instability of resistance is intrinsic to HR but is not currently part of the definition and thus is considered in few reports of HR (12).

In this report, we develop and analyze the properties of two mathematical and computer-simulation models that represent two extreme cases of HR, which we call progressive and non-progressive. Using these models, we explore the pharmaco- and population dynamic processes responsible for HR and the factors which contribute to the instability of HR. The parameters of these models can be estimated, and the hypotheses generated therefrom tested and rejected in vitro and in vivo.

Results

Models of Heteroresistance. We open this consideration of the pharmaco- and population dynamics of HR with a description of the two mathematical models employed. For both models of HR, we assume a Hill function for the relationship between the concentration of the antibiotic, the concentration of the limiting resource, and the rates of growth and death of the bacteria, known as the pharmacodynamics (13–15).

Pharmacodynamics. In accord with the Hill function, the net growth of bacteria exposed to a given antibiotic concentration is given by Eq. **1**.

$$\Pi_i(r, A) = \left(\nu_{\text{MAX}i} - \left[\frac{(\nu_{\text{MAX}i} - \nu_{\text{MIN}i}) \cdot \left(\frac{A}{\text{MIC}_i} \right)^{\kappa i}}{\left(\frac{A}{\text{MIC}_i} \right)^{\kappa i} - \left(\frac{\nu_{\text{MIN}i}}{\nu_{\text{MAX}i}} \right)} \right] \right) \cdot \psi(r),$$

[1]

where A in µg/mL is the antibiotic concentration, and r in µg/mL is the concentration of the resource which limits the growth of the population. $\nu_{\text{MAX}i}$ is the maximum growth rate in cells per hour of the bacteria of state i, where $\nu_{\text{MAX}i} > 0$. $\nu_{\text{MIN}i}$ is the minimum growth rate per cell per hour, which is the maximum death rate when exposed to the antibiotic, where $\nu_{\text{MIN}i} < 0$. MIC_i (which is >0) is the minimum inhibitory concentration of the antibiotic for the bacteria of state i in µg/mL. κi is the Hill coefficient for bacteria of state i. The greater the value of κi, the more acute the function. The Monod function (15), $\psi(r) = r/(r+k)$, is the rate of growth in the absence of the antibiotic, where k is the resource concentration in µg/mL when the growth rate is half of its maximum value. $\psi(r)$ measures the physiological state of the bacteria; as the resource concentration declines, the cells grow slower. We show in *SI Appendix*, Fig. S1 the Hill functions for four different bacterial populations with varying MICs and maximum growth rates.

Diagrams of the heteroresistance models. The two models of HR used here are depicted in Fig. 1. In the progressive model (Fig. 1*A*), the increasingly resistant states are generated by a transition from a less resistant state to a more resistant state, and the more resistant states generate the less resistant states sequentially. In the non-progressive model (Fig. 1*B*), the different resistant states are generated directly by a transition from the susceptible state, and the more resistant states transition directly back to the most sensitive state.

The progressive model. In this model (Fig. 1*A*), the bacteria transition between four different states: sensitive, *S*, and increasingly resistant, *R*1, *R*2, and *R*3, which are the designations and densities in cells per mL of bacteria of these different states. The total number of cells in a state is given by the product of the density of the state and the total volume, Vol. Cells of the *S* state
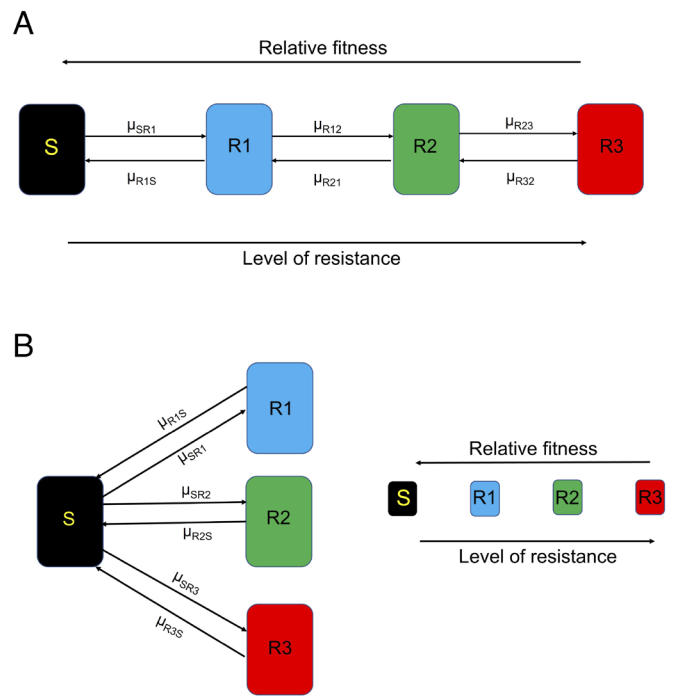
Fig. 1. Diagram of the two models of HR. *S* (black) is the most antibiotic-sensitive state and the state with the highest fitness. We assume that the level of antibiotic resistance increases as the fitness decreases from state *R*1 (blue) to *R*2 (green) to *R*3 (red). Transitions occur between states at potentially different rates of µ (where µ$_{ij}$ is the transition from i to j). Panel (*A*) is a diagram of the progressive model, and panel (*B*) is a diagram of the non-progressive model.

transition to *R*1, *R*1 transitions to *R*2, and *R*2 transitions to *R*3 at rates µ$_{S1}$, µ$_{R12}$, and µ$_{R23}$ per cell per hour, respectively. Cells of resistant states progressively transition to the less resistant states, *R*3 to *R*2, *R*2 to *R*1, and *R*1 to *S*, with rates µ$_{R32}$, µ$_{R21}$, and µ$_{R1S}$ per cell per hour. We simulate these transitions with a Monte Carlo process to account for the stochasticity that occurs during cell division related to either gene amplification or a point mutation at a specific locus due to the polymerase error rate (16). In this Monte Carlo process, a pseudorandom number x (0 ≤ x ≤1) is generated from a rectangular distribution (17). If x is less than the product of the total number of cells in the generating state, the transition rate (µ), the Monod function ($\psi(r)$), and the step size (dt) of the Euler method (18) employed for solving differential equation, then 1/(dt*Vol) cells are added to the recipient population and removed from the generating population. In the equations below, the transition of cells due to this process is expressed as MIJ, e.g., MR1S for transitions from *R*1 to *S* and MR21 for transitions from *R*2 to *R*1. For example, if *S* is 10^5, µ$_{SR1}$ is 10^{-7}, dt is 10^{-4}, Vol is 1, and x < *S**µ$_{SR1}$**dt**Vol* $\psi(r)$, which in this case is 10^{-6}* $\psi(r)$, then 1/(dt*Vol) cells are removed from the S population and added to the R1 population, which in this case would mean that MSR1 is 10^4 cells. Practically, when MSR1 is plugged into the differential equations below, it means that for any given step of the Euler method from t to $t + dt$ we add (1/(dt*Vol))*dt cells, so here, there would be one cell added. In this model the assumption that there are 1 sensitive and 3 resistant states is arbitrary, but in reality, there could be more or fewer states depending on the mechanism of HR. In the simulations presented in the main text, we assume the transition rates between states are equal in both directions and between states. We also assume that the transitions between states slow down with the decline in the physiological state of the cells in direct proportion to $\psi(r)$. With these definitions, assumptions,

and the parameters defined and presented in *SI Appendix,* Table S1, the rates of change in the densities of the different populations are given by,

$$\frac{dr}{dt} = \underbrace{-e \cdot \psi(r) \cdot \left(\nu_S \cdot S + \nu_1 \cdot R1 + \nu_2 \cdot R2 + \nu_3 \cdot R3\right),}_{\text{Rate of consumption of the limiting resource}} \quad [2]$$

$$\frac{dS}{dt} = \underbrace{S \cdot \Pi_S(r, A)}_{\text{Growth of } S} + \underbrace{MR1S - MSR1}_{\text{Monte Carlo Transitions}}, \quad [3]$$

$$\frac{dR1}{dt} = \underbrace{R1 \cdot \Pi_{R1}(r, A)}_{\text{Growth of } R1} + \underbrace{MSR1 + MR21 - MR12 - MR1S,}_{\text{Monte Carlo Transitions}} \quad [4]$$

$$\frac{dR2}{dt} = \underbrace{R2 \cdot \Pi_{R2}(r, A)}_{\text{Growth of } R2} + \underbrace{MR12 + MR32 - MR21 - MR23,}_{\text{Monte carlo Transitions}} \quad [5]$$

$$\frac{dR3}{dt} = \underbrace{R3 \cdot \Pi_{R3}(r, A)}_{\text{Growth of } R3} + \underbrace{MR23 - MR32}_{\text{Monte carlo Transitions}}. \quad [6]$$

The non-progressive model. In this model (Fig. 1*B*), all the resistant states, $R1$, $R2$, and $R3$ are derived from the susceptible state and, by transition, return directly to the susceptible state, S. The rates of transition from state S are, respectively, μ_{SR1}, μ_{SR2}, and μ_{SR3} per cell per hour. The rates of return to the susceptible state are μ_{R1S}, μ_{R2S}, and μ_{R3S} per cell per hour. The transitions between states are via a Monte Carlo process (16), using a routine like that for the progressive model. When transients from S to the different R states are generated (MSR1, MSR2, and MSR3), 1/(dt*Vol) are added to the $R1$, $R2$, and $R3$ populations and are removed from the S population. When transients from the $R1$, $R2$, and $R3$ populations are generated (MR1S, MR2S, and MR3S), 1/(dt*Vol) are added to the S population and removed from the $R1$, $R2$, and $R3$ populations, respectively. Here, the primary assumption is that all resistant states are derived from and transition back to the sensitive state and we continue to assume there are four states with equal transition rates between them. With these definitions, assumptions, and the parameters defined and presented in *SI Appendix,* Table S1, the rates of change in the densities of the different populations are given by:

$$\frac{dr}{dt} = \underbrace{-e \cdot \psi(r) \cdot \left(\nu_S \cdot S + \nu_1 \cdot R1 + \nu_2 \cdot R2 + \nu_3 \cdot R3\right),}_{\text{Rate of consumption of the limiting resource}} \quad [7]$$

$$\frac{dS}{dt} = \underbrace{S \cdot \Pi_S(r, A)}_{\text{Growth of } S} - \underbrace{MSR1 - MSR2 - MSR3 + MR1S + MR2S + MR3S,}_{\text{Monte Carlo Transitions}} \quad [8]$$

$$\frac{dR1}{dt} = \underbrace{R1 \cdot \Pi_{R1}(r, A)}_{\text{Growth of } R1} + \underbrace{MSR1 - MR1S}_{\text{Monte Carlo Transitions}}, \quad [9]$$

$$\frac{dR2}{dt} = \underbrace{R2 \cdot \Pi_{R2}(r, A)}_{\text{Growth of } R2} + \underbrace{MSR2 - MR2S}_{\text{Monte Carlo Transitions}}, \quad [10]$$

$$\frac{dR3}{dt} = \underbrace{R3 \cdot \Pi_{R3}(r, A)}_{\text{Growth of } R3} + \underbrace{MSR3 - MR3S}_{\text{Monte Carlo Transitions}}. \quad [11]$$

Simulated Population Dynamics of Heteroresistance. Here, we consider the population dynamics of HR with the distributions of the different resistant states generated from single cells grown up to full densities for the progressive and non-progressive models with four transition rates (Fig. 2). We further consider a greater range of transition rates for the non-progressive model to determine the minimum rate for which we generate sufficiently large minority populations in *SI Appendix,* Fig. S2 *A–C*.

For the progressive model, only in the runs with the highest transition rates, $\mu = 10^{-2}$ and $\mu = 10^{-3}$ per cell per hour, is the subpopulation with the highest resistance level, $R3$, present. A very different situation obtains for the non-progressive model, as at every transition rate the $R3$ population is present. We also consider the effect that the relative fitness cost of each state has on these stationary phase densities (*SI Appendix,* Fig. S3) and find modest differences in these distributions.

Using these same parameters for both models, another difference can be seen between the progressive and non-progressive models in the PAP tests of each (Fig. 3). For these PAP tests, we calculate the ratio of the number of cells generated at a particular antibiotic concentration compared to the number of cells present when there is no antibiotic [N(A)/N(0)] for 0, 1, 2, 4, 8, and 16 times the MIC of the susceptible population.

The PAP test results anticipated from the progressive model are very different than those anticipated from the non-progressive model, two extreme HR cases. The presence of four subpopulations with different MICs is apparent from the PAP test of the progressive model with the parameters considered. For the non-progressive model, the differences in the relative densities of the subpopulations are too low to be detected by a PAP test performed in the lab. In general, the plateaus shown in Fig. 3 *A* and *B* are sharper and more dramatic than would be seen in the lab. This is a consequence of having only three resistant states. Moreover, using the standard HR criteria of having a subpopulation with an MIC of >8 times at a frequency of at least 10^{-7}, the progressive model only meets these criteria at high transition rates (exceeding 10^{-4}). On the other hand, the non-progressive model meets these criteria at transition rates as low as 10^{-7} (*SI Appendix,* Fig. S2D).

To explore how these models differ in their response to antibiotic treatment, we follow the changes in the densities and MICs of heteroresistant populations exposed to two antibiotic concentrations (5 μg/mL and 10 μg/mL corresponding to 5× and 10× the MIC of the susceptible population) when $\mu = 10^{-2}$ and $\mu = 10^{-5}$ per cell per hour (*SI Appendix,* Fig. S4). We initiate these simulations with 1/100 of the stationary phase densities of the different states anticipated from the heteroresistant populations depicted in Fig. 2 *A, D, H,* and *E* for the progressive and non-progressive models of heteroresistance, respectively. In *SI Appendix,* Fig. S5, we consider the effect that the fitness cost of resistance has on these dynamics and find the effect modest at best, just slowing the response time to the antibiotic.
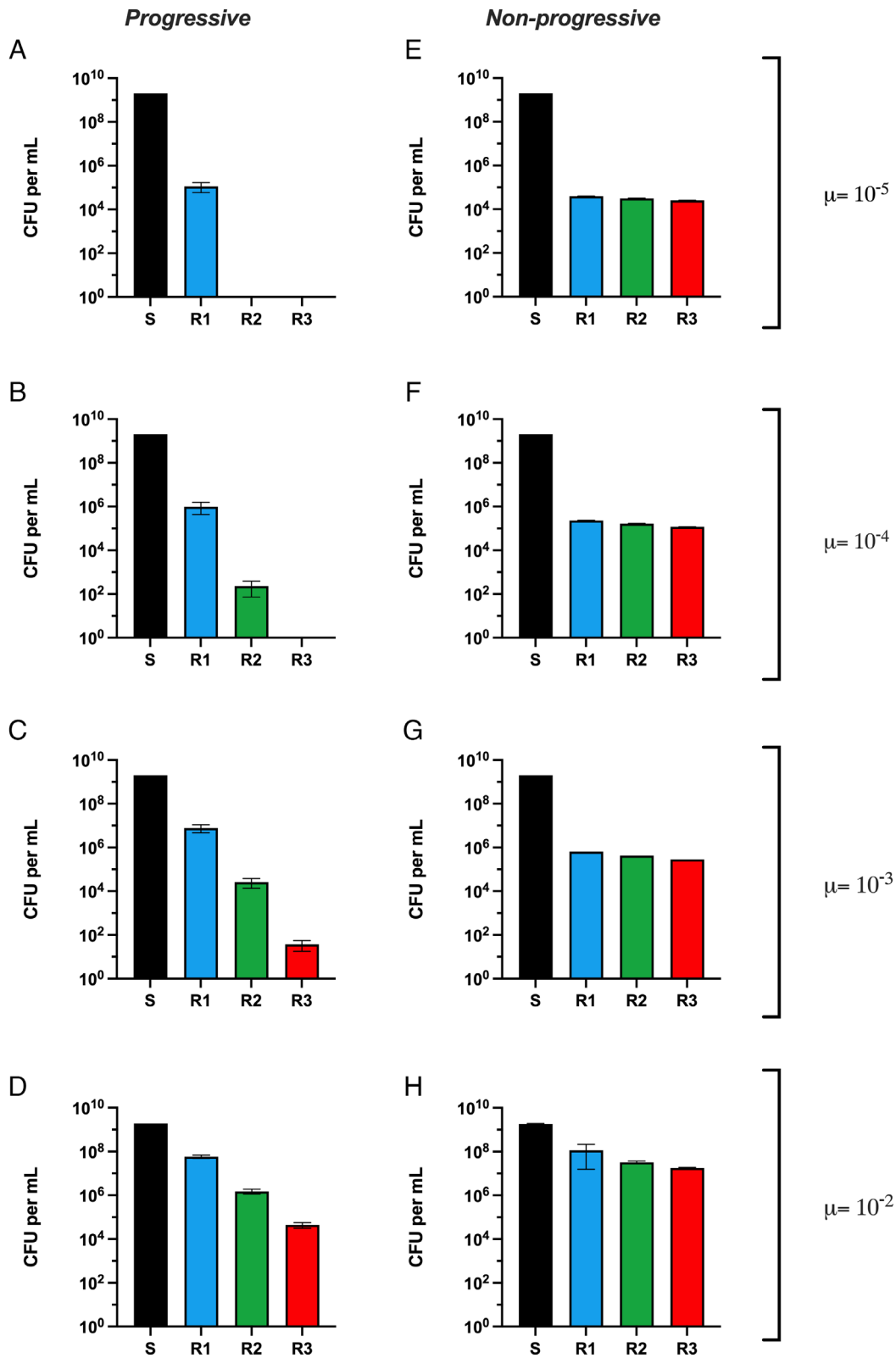
Progressive   *Non-progressive*

Fig. 2. Distribution of stationary phase densities when grown up from a single cell of *S*. Shown on the *Left* (*A–D*) are the means and SDs of the stationary phase densities of the *S* (black), *R*1 (blue), *R*2 (green), and *R*3 (red) populations from five independent runs with the progressive model with different transition rates, $\mu = 10^{-5}$, 10^{-4}, 10^{-3} and 10^{-2} per cell per hour for (*A–D*), respectively. On the *Right*, (*E–H*) are the corresponding distributions for runs made with the non-progressive model with these respective transition rates.

There are apparent differences in the bacterial response to antibiotics between the progressive and non-progressive models of HR. For both models, when $\mu = 10^{-2}$ per cell per hour, the *R*3 population comes to dominate and the MIC increases to the maximum (15 μg/mL), though with the higher concentration of the drug, it takes longer for the *R*3 population to become dominant. With the lower transition rate of $\mu = 10^{-5}$ per cell per hour, at 5 μg/mL of antibiotic, the *R*2 population comes to dominate in the progressive
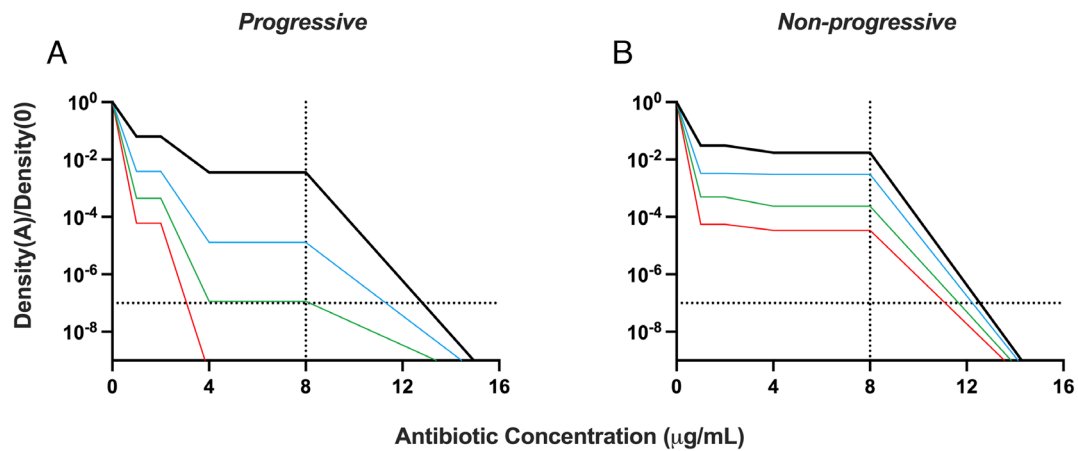
Fig. 3. PAP tests. The ratio of the density of the number of bacteria surviving at an antibiotic concentration relative to that surviving in the absence of the antibiotic for different transition rates. Black $\mu = 10^{-2}$, blue $\mu = 10^{-3}$, green $\mu = 10^{-4}$, and red $\mu = 10^{-5}$ per cell per hour. Panel (*A*) is the PAP test using the progressive model, and panel (*B*) is the PAP test using the non-progressive model.

model and the *R*3 population remains minor. At this same transition rate and at 10 μg/mL, resistance does not evolve, and the bacterial populations are lost. In both cases, the MIC does increase but does not go to the maximum value. For these conditions, in the non-progressive model, subpopulations are always able to respond to the antibiotic and are never eliminated.

Upon removal of the antibiotic, the heteroresistant bacterial population reverts to the sensitive state. This reversion is the case for both the progressive and non-progressive models of HR considered here. To illustrate this and elucidate the relative contributions of the rates of transition between states and the fitness cost of resistance (as measured by the growth rates) to the dynamics and the time needed to restore susceptibility, we use serial transfer forms of the progressive and non-progressive versions of the HR models. In these simulations, the populations are grown for 24 h, diluted by a factor of 100, and fresh resources added. In Fig. 4, we present the results of simulations of the changes in the densities of the susceptible and resistant populations as well as the change in average MIC in serial transfer following the removal of the antibiotics. These serial transfer simulations were initiated with 10^7 bacteria per mL of the highest resistance level, *R*3. We consider two major conditions: one where the fitness cost of resistance is high and another where the fitness cost of resistance is low. In *SI Appendix*, we consider the dynamics of reversion when a set of even higher fitness costs are used (*SI Appendix,* Fig. S6).

In the absence of antibiotics, the populations become increasingly dominated by more susceptible populations for both the progressive and non-progressive models of HR. This change in the composition of the populations is also reflected in a decline in the average MIC, approaching the level of the susceptible population. With the same fitness parameter and transition rates between states, μ, the rate of return to the susceptible state is greater for the non-progressive model than the progressive model. For both models, the rate of return to the sensitive state is proportional to the transition rate between states, μ, and the relative fitness cost of resistance. Notably, the new apparent equilibria obtained for both models differ substantially. In the progressive model, the most resistant populations are in continuous decline and will ultimately be lost or nearly so, while in the non-progressive model, all resistant populations are present at roughly equal frequency and appear to be in equilibrium. Of note is the vast difference in the time needed for the susceptible population to come to dominate; we list these times in *SI Appendix*, Table S2.

Discussion

To elucidate the factors that govern the response of heteroresistant populations to antibiotics, we use mathematical and computer-simulation models to explore quantitatively: i) the factors responsible for generating the distribution of resistant subpopulations, ii) the response of heteroresistant populations to different concentrations of antibiotics, and iii) the amount of time required for an antibiotic-resistant heteroresistant population to become susceptible again when the treating antibiotic is removed.

We consider two models of heteroresistance (HR), which we call progressive and non-progressive. In both models, there are one or more subpopulations with different levels of resistance. In the progressive model, the more susceptible state transitions sequentially to the more resistant states, which in turn transition back to the less resistant states in the same sequence. In the non-progressive model, the susceptible population transitions directly to all the resistant states from the susceptible state before transitioning back directly to the susceptible state. In both models, the transition rates between states and the relative fitness cost of being resistant determine the distribution of the resistant populations in the absence of and in response to antibiotics.

The difference in the distribution of resistant states between these models with the parameters used is apparent with a PAP test. With the progressive model, there are different resistance levels with distinct relative densities, which decline as the concentration of the antibiotic increases. With the non-progressive model, although there are multiple subpopulations with different levels of resistance, they likely would not appear as separate populations in a PAP test. The PAP test of the non-progressive HR looks more like that which would obtain with only two resistance levels, sensitive and resistant. However, the PAP tests are insufficient to differentiate the two models of HR, as there are conditions where non-progressive HR would look progressive (*SI Appendix,* Fig. S7).

The models are also distinct in how they respond to antibiotics. In the progressive model, if the drug concentration is above the MIC of any of the subpopulations and the transition rate is low, the most resistant population can fail to emerge and ascend; this is true even though the drug concentration is still less than the MIC of the most resistant population. With the non-progressive model, the highest level of resistance will always emerge, no matter the transition rate. There are also differences in the population dynamics of each model when the antibiotics are removed. In the
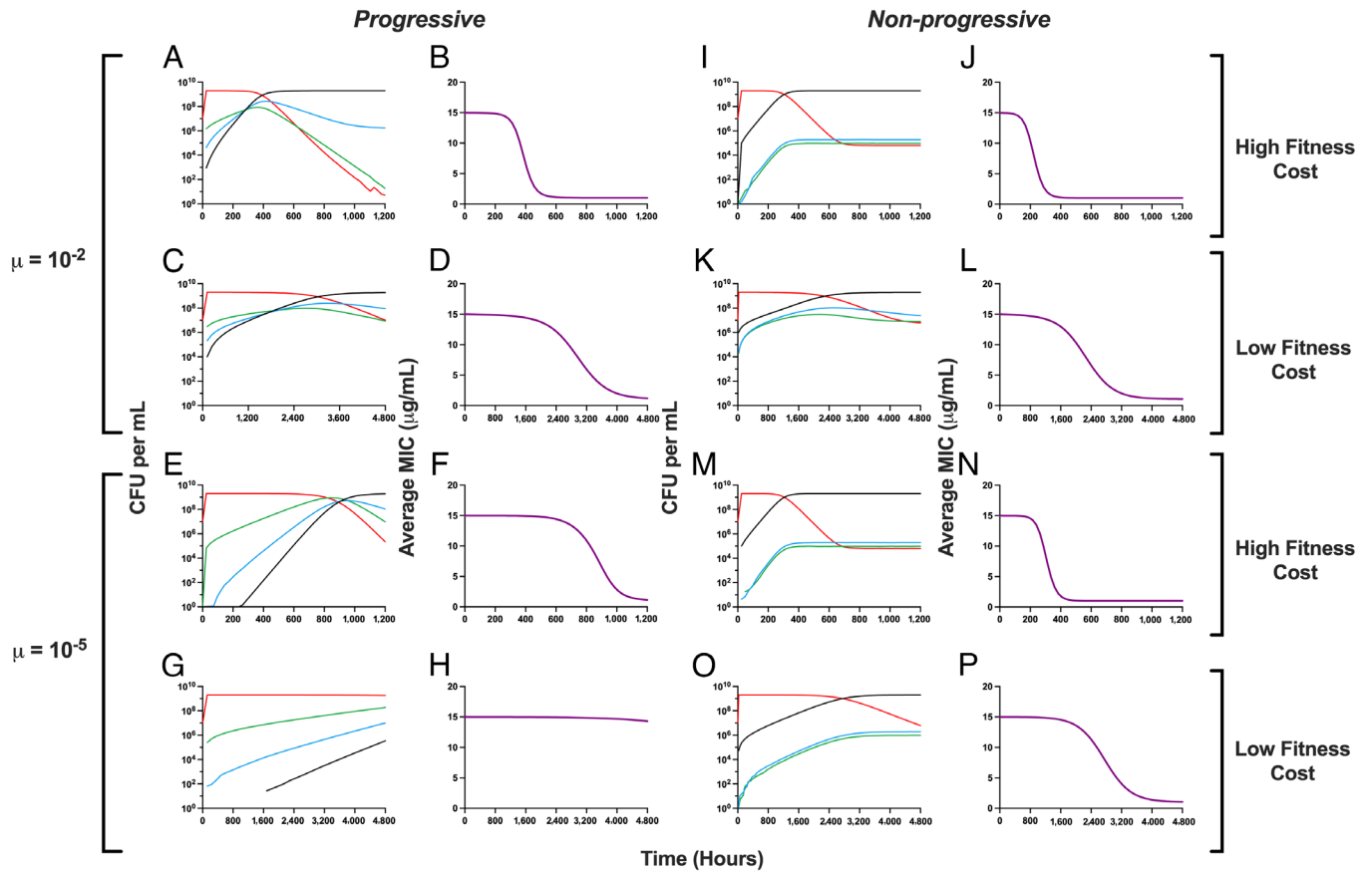
Fig. 4. Response of the two heteroresistant models to the removal of antibiotics. Changes in the densities of the susceptible and resistant populations in the absence of the antibiotic and changes in the average MIC. *S* (black), *R*1 (blue), *R*2 (green), and *R*3 (red). Simulations with the high fitness cost were run for 1,200 h (50 d), while simulations with the low fitness cost were run for 4,800 h (200 d). *A-H*, predictions of the Progressive model. *I-P*, predictions of the Non-progressive model. *A, C, E, G, I, K, M,* and *O* are changes in the density of each bacterial population that occurs over time when the antibiotic is removed. *B, D, F, H, J, L, N,* and *P* are changes in the average MIC of each condition over time when the antibiotic is removed.

progressive model, the average MIC will return to that of the most susceptible population, and the most resistant populations will be lost. In contrast, in the non-progressive model, the average MIC will not decrease to that of the most susceptible population, and all the resistant subpopulations will remain present. One implication of this is when confronted with antibiotics, a heteroresistant population which is non-progressive will respond to the drugs more consistently and more rapidly than a progressive heteroresistant population.

The standard for detecting and defining a strain as heteroresistant is the PAP test which requires subpopulations to be more frequent than 10^{-7} and to have an MIC >8× that of the susceptible main population (9). These tests are cumbersome, costly, and are unlikely to be performed in clinical microbiology labs. Most critically, our results demonstrate that the PAP test is not sufficient to detect HR. There are conditions with the progressive and non-progressive models where populations would fail to meet the criteria set by the PAP test but would still survive confrontation with high doses of antibiotics—a false negative (*SI Appendix,* Fig. S2D). There are also conditions where stable resistance would meet the HR criteria set by the PAP test—a false positive (*SI Appendix,* Fig. S8). The resistance that occurs in *SI Appendix,* Fig. S8 is a canonical point mutation in *rpoB* which does not have a fitness cost and will not revert (19). Moreover, there are conditions that would be called HR despite requiring thousands of hours to return to a sensitive MIC. These results point to both a failing of the PAP test and to the insufficiency of the operational definition

of HR. To address the definitional issue, we recommend revisiting this operational definition to include the rate at which the MIC of potentially heteroresistant strains return to a susceptible MIC as proposed in our model to better capture the underlying biology of HR (12). This is especially important, as the epidemiological risk of HR is the rapid return to a seemingly sensitive state, and as demonstrated experimentally, this can happen in less than 50 generations for certain types of HR (12, 20, 21).

At this juncture, it is not clear how important HR is clinically even though animal experiments (22, 23) and some clinical studies suggest that it can increase the risk of persistent bacteremia, lead to longer hospital stays, and increase mortality (12). We argue that within a single infected individual, the distinction between the emergence of stable resistance and HR is manifest in the risk of treatment failure. With both mechanisms, antibiotics can select for the ascent of resistant subpopulations which will result in reduced treatment efficacy or even treatment failure, likely leading clinicians to change the treating drug in both cases. This risk of treatment failure is probabilistic in HR, as it is in stable resistance, due to other factors not considered here such as the host's immune system, the compartmental heterogeneity and the chronicity of infection, the total density of infecting bacteria, and the local antibiotic concentrations. Due to the combination of these factors, treatment of a heteroresistant strain with a drug for which it is heteroresistant, will not necessarily lead to treatment failure. One distinction between HR and stable resistance is the rapid reversion of a heteroresistant population from a resistant to a susceptible state. This reversion has an additional clinical implication

when considering infection transmission between individuals. Should an individual be infected with bacteria that are stably resistant to a drug, that resistance would appear on an assay such as the VITEK, and the drug for which they are resistant would not be used. If that individual is infected with heteroresistant bacteria, it would initially appear sensitive to a treating drug, but resistance could rapidly ascend. Then if that individual passes the infection on to another individual, due to the transient nature of HR, that infection would once again appear susceptible to the drug and once again the wrong drug would be chosen to treat the infection.

Although this study is purely theoretical, the parameters used in these models can be estimated experimentally with different species of bacteria and antibiotics of different classes. The hypotheses generated herein can be tested in vitro and, most importantly, can be rejected. There exists evidence supporting these two classes of HR, primarily in the form of PAP tests of known heteroresistant strains as exemplified by data shown in *SI Appendix,* Fig. S9. A key objective for future experimental work is to determine how the actual mechanisms that can generate an unstable heteroresistant phenotype relate to these theoretical models. At present, we know of two main mechanisms that can generate HR: i) alterations in copy number of resistance genes or their regulators by either tandem amplifications and/or alterations in plasmid copy number (12, 20, 24, 25) and ii) regular point mutations that occur at a high frequency (20, 26–28). It is likely that mutational HR is best described by the non-progressive model where instability and reversion to susceptibility is driven by compensatory mutations that concomitantly reduce the fitness costs of the resistance mutations and lead to the loss of resistance (29–31). For gene amplification mechanisms it is less clear which theoretical model best describes their behavior since these mechanisms could have properties compatible with either model alone or a combination of the two, depending on the actual mechanism by which the amplifications are formed and lost. Further experimental work is needed to clarify these points. Finally, an unstable and transient resistant minority population could potentially also be generated by other types of mechanisms than those presently identified, including inducible resistances, epigenetic changes, and gene conversion events (32).

While our models are agnostic to mechanism and to the underlying bacteria and antibiotic, ultimately, we are interested in and believe our results have clinical implications for the design and implementation of antibiotic treatment regimens. For example, in bacteria such as *Escherichia coli, Klebsiella pneumoniae, Acinetobacter baumannii,* and *Staphylococcus aureus,* mutations in genes involved in, for example, electron transport, cell wall biosynthesis, and two-component regulatory systems, can lead to resistance to colistin, gentamicin, oxacillin, daptomycin, and teicoplanin (18, 24–26, 33). These types of mutations, which are difficult to detect under standard susceptibility testing conditions, could lead to the rapid emergence of resistance in vivo—which would be a type of non-progressive HR. Progressive HR also necessarily starts by single events which are not detectable in antibiotic susceptibility testing, but only reach clinically relevant levels of resistance after several events, as seen with stepwise gene amplifications of various genes conferring resistance to β-lactams, aminoglycosides, colistin, and tetracyclines (24–26, 30). The impact of the reversion rate to the treatment of infected individuals is difficult to evaluate in acute infections. However, the importance of the reversion rate is critical for understanding the level of antibiotic resistance. In *SI Appendix, Supplemental Text* and Table S3, we provide examples of mechanisms across several drug classes that have been shown to or could hypothetically generate an HR phenotype, predict which model of HR would most accurately pertain, and discuss further clinical implications.

There are, of course, caveats to consider with our models. First, our models are not mechanistic and do not consider the genetic basis of progressive versus non-progressive HR, and, as mentioned above, there are likely cases where certain mechanisms (e.g., gene amplification) could look either progressive, non-progressive, or somewhere in between depending on their specific mechanistic properties. Second, our models only include three resistant states, and these resistant states either do not transition between each other (non-progressive) or transition sequentially (progressive)—two extreme cases. Last, as with all pharmacodynamic studies, some elements have been neglected from these models, as mentioned previously, the host's immune system and the compartmental heterogeneity of infection such as biofilms and abscesses, as well as variation in local antibiotic concentrations, all of which prohibit in vitro models and studies from making solid clinical predictions. All in all, a clear next step would be to test these predictions in vitro and then move to an in vivo model system. Crucially, we need to develop an understanding of how the definition of HR matches with the clinical implications, specifically considering the frequency and MIC cutoffs previously defined.

Materials and Methods

Numerical Solutions (Simulations). For our numerical analysis of the coupled, ordered differential equations presented (Eqs. **2**–**11**), we used Berkeley Madonna with the parameters presented in *SI Appendix,* Table S1. Copies of the Berkeley Madonna programs used for these simulations are available at https://www.eclf.net. In the analysis of our simulations, to calculate average MIC, we take a weighted average of the MIC of each population.

Bacteria. *Enterobacter cloacae* Mu208 is a carbapenem-resistant isolate collected by the Georgia Emerging Infections Program Multi-site Gram-negative Surveillance Initiative and described previously (23). *Burkholderia cepacia* complex isolate JC8 is a cystic fibrosis patient isolate collected by the Georgia Emerging Infections Program Multi-site Gram-negative Surveillance Initiative. *E. coli* MG1655 was obtained from the Levin Lab's bacterial collection.

Rifampin PAP Tests. Single colonies of *E. coli* MG1655 were inoculated into 10 mL lysogeny broth (BD, Product #244610) and grown overnight at 37 °C with shaking. Cultures were serially diluted in saline and all dilutions (10^0 to 10^{-7}) plated on LB agar plates (BD, Product #244510) containing 0, 1, 2, 4, 8, and 16 times the MIC of rifampin (Thermo Fisher, Product #J60836.03). Plates were grown at 37 °C for 48 h before the density of surviving colonies was estimated.

Burkholderia and Enterobacter PAP Tests. Single colonies of *B. cepacia* complex isolate JC8 and *E. cloacae* Mu208 were inoculated into 1.5 mL Mueller–Hinton broth (BD, Product #275730), and cultures were grown overnight at 37 °C with shaking. Cultures were serially diluted in phosphate-buffered saline, and 10 µL of each dilution was spotted on Mueller–Hinton agar (BD, Product #225250) plates containing 0, 0·125, 0.25, 0·5, 1, 2, and 4 times the breakpoint concentration of each antibiotic. Antibiotics used were ticarcillin disodium (BioVision, Product #B1536) with clavulanate potassium salt (Cayman Chemical Company, Procut #19456), amikacin sulfate (AstaTech, Product # 40003), colistin sulfate salt (Sigma-Aldrich, Product # C4461), and fosfomycin disodium salt (TCI America, Product # F0889). For Mu208 on fosfomycin, broth and agar included 25 µg/mL glucose-6-phosphate (Sigma-Aldrich, Product #10127647001). Plates were maintained at 37 °C overnight for Mu208 and for 36 to 60 h for JC8.

Author affiliations: [a]Department of Biology, Emory University, Atlanta, GA 30322; [b]Emory Antibiotic Resistance Center, Atlanta, GA 30322; [c]Program in Microbiology and Molecular Genetics, Graduate Division of Biological and Biomedical Sciences, Laney Graduate School, Emory University, Atlanta, GA 30322; [d]Emory Vaccine Center, Atlanta, GA 30322; [e]Department of Medical Biochemistry and Microbiology, Uppsala University, Uppsala SE-75123, Sweden; [f]Division of Infectious Diseases, Department of Medicine, Emory University School of Medicine, Atlanta, GA 30322; [g]Georgia Emerging Infections Program, Georgia Department of Public Health, Atlanta, GA 30322; and [h]Servicio de Microbiología, Hospital Universitario Ramón y Cajal, Instituto Ramón y Cajal de Investigación Sanitaria, and Centro de Investigación Biomédica en Red Epidemiología y Salud Pública, Madrid 28034, Spain

1. B. Bengtsson, C. Greko, Antibiotic resistance–consequences for animal health, welfare, and food production. *Ups J. Med. Sci.* **119**, 96–102 (2014).
2. C. J. L. Murray *et al.*, Global burden of bacterial antimicrobial resistance in 2019: A systematic analysis. *The Lancet* **399**, 629–655 (2022).
3. A. P. MacGowan, R. Wise, Establishing MIC breakpoints and the interpretation of in vitro susceptibility tests. *J. Antimicrob. Chemother.* 48 (Suppl 1), 17–28 (2001).
4. R. Humphries, A. M. Bobenchik, J. A. Hindler, A. N. Schuetz, Overview of changes to the clinical and laboratory standards institute performance standards for antimicrobial susceptibility testing. *J. Clin. Microbiol.* **59**, e0021321 (2021).
5. M. Bardelli *et al.*, A side-by-side comparison of the performance and time-and-motion data of VITEK MS. *Eur. J. Clin. Microbiol. Infect Dis.* **41**, 1115–1125 (2022).
6. Anonymous, Comité de l'Antibiogramme de la Société Française de Microbiologie report 2003. *Int. J. Antimicrob. Agents* **21**, 364–391 (2003).
7. H. M. Ericsson, J. C. Sherris, Antibiotic sensitivity testing. Report of an international collaborative study. *Acta Pathol. Microbiol. Scand B. Microbiol. Immunol.* 217 (suppl 217), 211 + (1971).
8. D. F. Brown, L. Brown, Evaluation of the E test, a novel method of quantifying antimicrobial activity. *J. Antimicrob. Chemother.* **27**, 185–190 (1991).
9. M. E. Falagas, G. C. Makris, G. Dimopoulos, D. K. Matthaiou, Heteroresistance: A concern of increasing clinical significance? *Clin. Microbiol. Infect* **14**, 101–104 (2008).
10. K. Hiramatsu *et al.*, Dissemination in Japanese hospitals of strains of Staphylococcus aureus heterogeneously resistant to vancomycin. *Lancet* **350**, 1670–1673 (1997).
11. O. M. El-Halfawy, M. A. Valvano, Antimicrobial heteroresistance: An emerging field in need of clarity. *Clin. Microbiol. Rev.* **28**, 191–207 (2015).
12. D. I. Andersson, H. Nicoloff, K. Hjort, Mechanisms and clinical relevance of bacterial heteroresistance. *Nat. Rev. Microbiol.* **17**, 479–496 (2019).
13. R. R. Regoes *et al.*, Pharmacodynamic functions: A multiparameter approach to the design of antibiotic treatment regimens. *Antimicrob. Agents Chemother.* **48**, 3670–3676 (2004).
14. B. A. Berryhill *et al.*, What's the matter with MICs: Bacterial nutrition, limiting resources, and antibiotic pharmacodynamics. *Microbiol. Spectr.* **11**, e0409122 (2023).
15. J. Monod, The growth of bacterial cultures. *Annu. Rev. Microbiol.* **3**, 371–394 (1949).
16. N. Metropolis, S. Ulam, The Monte Carlo Method. *J. Am. Statis. Assoc.* **44**, 335–341 (1949).
17. J. E. Gentle, *Random Number Generation and Monte Carlo Methods* (Springer, 1998).
18. G. Wanner, E. Hairer, *Solving Ordinary Differential Equations II* (Springer, Berlin Heidelberg New York, 1996), **vol. 375**.
19. M. G. Reynolds, Compensatory evolution in rifampin-resistant Escherichia coli. *Genetics* **156**, 1471–1481 (2000).
20. H. Nicoloff, K. Hjort, B. R. Levin, D. I. Andersson, The high prevalence of antibiotic heteroresistance in pathogenic bacteria is mainly caused by gene amplification. *Nat. Microbiol.* **4**, 504–514 (2019).
21. C. Pereira, J. Larsson, K. Hjort, J. Elf, D. I. Andersson, The highly dynamic nature of bacterial heteroresistance impairs its clinical detection. *Commun. Biol.* **4**, 521 (2021).
22. V. I. Band *et al.*, Carbapenem-resistant Klebsiella pneumoniae exhibiting clinically undetected colistin heteroresistance leads to treatment failure in a murine model of infection. *mBio* **9**, e02448-17 (2018).
23. V. I. Band *et al.*, Antibiotic combinations that exploit heteroresistance to multiple drugs effectively control infection. *Nat. Microbiol.* **4**, 1627–1635 (2019).
24. K. Hjort, H. Nicoloff, D. I. Andersson, Unstable tandem gene amplification generates heteroresistance (variation in resistance within a population) to colistin in Salmonella enterica. *Mol. Microbiol.* **102**, 274–289 (2016).
25. S. E. Anderson, E. X. Sherman, D. S. Weiss, P. N. Rather, Aminoglycoside Heteroresistance in Acinetobacter baumannii AB5075. *mSphere* **3**, e00271-18 (2018).
26. Y. Charretier *et al.*, Colistin heteroresistance and involvement of the PmrAB regulatory system in Acinetobacter baumannii. *Antimicrob. Agents Chemother.* **62**, e00788-18 (2018).
27. T. Halaby *et al.*, Genomic characterization of colistin heteroresistance in Klebsiella pneumoniae during a nosocomial outbreak. *Antimicrob. Agents Chemother.* **60**, 6837–6843 (2016).
28. A. Jayol, P. Nordmann, A. Brink, L. Poirel, Heteroresistance to colistin in Klebsiella pneumoniae associated with alterations in the PhoPQ regulatory system. *Antimicrob. Agents Chemother.* **59**, 2780–2784 (2015).
29. D. I. Andersson, B. R. Levin, The biological cost of antibiotic resistance. *Curr. Opin. Microbiol.* **2**, 489–493 (1999).
30. D. I. Andersson, D. Hughes, Antibiotic resistance and its cost: Is it possible to reverse resistance? *Nat. Rev. Microbiol.* **8**, 260–271 (2010).
31. R. C. Allen, J. Engelstädter, S. Bonhoeffer, B. A. McDonald, A. R. Hall, Reversing resistance: Different routes and common themes across pathogens. *Proc. Biol. Sci.* **284**, 20171619 (2017).
32. V. G. Meka *et al.*, Reversion to susceptibility in a linezolid-resistant clinical isolate of Staphylococcus aureus. *J. Antimicrob. Chemother.* **54**, 818–820 (2004).
33. S. Heidarian, A. Guliaev, H. Nicoloff, K. Hjort, D. I. Andersson, High prevalence of heteroresistance in Staphylococcus aureus is caused by a multitude of mutations in core genes. *PLoS Biol.* **22**, e3002457 (2024).
34. B. R. Levin, Escherichia coli Liberation Front, Programs. ECLF.NET. https://www.eclf.net. Accessed 1 March 2024.